journal

J. Am. Ceram. Soc., 78 [9] 2367-73 (1995)

Preventing Segregation during Centrifugal Consolidation of Particulate Suspensions: Particle Drafting

Ryan K. Roeder,* Greg A. Steinlage, Kevin P. Trumble,* and Keith J. Bowman*

School of Materials Engineering, Purdue University, West Lafayette, Indiana 47907

Dilute, dispersed, multicomponent suspensions containing Ce-ZrO_2, Al_2O_3, and varying Al_2O_3-platelet contents were centrifugally consolidated. Despite the favorable conditions for segregation, phase and size segregation did not occur in the highest Al_2O_3-platelet content suspension. The suspension properties did not consist of agglomeration, high solids fractions, or high suspension viscosities typically attributed with segregation prevention. Thus, a new mechanism is suggested, considering the effects of hydrodynamic particle interactions (interference drag or "drafting") on particle arrangement during consolidation. Particle drafting is proposed and supported as a mechanism for preventing segregation, and the importance of hydrodynamic particle interactions in ceramic processing is discussed.

I. Introduction

Overcoming the seemingly inherent tradeoff between consolidation behaviors for dispersed and agglomerated (flocculated or coagulated) suspensions has been paramount to developing colloidal routes for producing ceramics and especially ceramic composites. Typical consolidation behavior for a dispersed suspension includes high particle packing densities and segregation by size or density. Conversely, lower particle packing densities and uniform microstructures are typically associated with agglomerated suspensions. The desire to produce dense, uniform microstructures leads to the necessity of preventing segregation in dispersed suspensions or increasing particle packing density in agglomerated suspensions. While most research has utilized agglomeration as a sure means of preventing segregation, the requirements and mechanisms for preventing segregation in a dispersed suspension remain uncertain.

Conventional mechanisms for preventing segregation fall into the following categories: agglomeration, high solids fractions, high suspension viscosities, and high consolidation rates. In agglomeration, interparticle surface forces are manipulated such that attractive interparticle forces cause particles to group together. Thus, the resultant agglomerates overcome differences in the sedimentation rates of individual particles to prevent segregation. Attractive interparticle forces can be accomplished by flocculation and heteroflocculation,[1-6] and by coagulation and heterocoagulation.[6-10] Sol–gel processing offers another means whereby agglomeration can be used to avoid segregation.[11]

A high solids fraction (usually >40 vol%) increases the effective suspension viscosity, thereby preventing segregation.[12-16] As the number density of particles increases, conditions can be reached where interparticle repulsions become interactive. Consolidation can be thought of as a moving "network" of dispersed particles, wherein segregation of faster settling particles is hindered by repulsions with slower settling particles. Furthermore, as the solids fraction increases, the particles have less distance to travel and segregate before being consolidated. In other fields, this same mechanism of preventing segregation at high solids fraction has been termed "hindered settling."[17-21]

High suspension viscosities can inhibit segregation by increasing the resistance to particle motion in the liquid medium. Suspension viscosities can be increased by agglomeration, increased solids loading and polymer additives.[22,23] Thus, suspension viscosity is often partly responsible for preventing segregation by agglomeration or high solids loading.

Faster consolidation rates have also been noted for preventing segregation, but conclusive experimental evidence and mechanisms have not been described. In the work of Sacks *et al.*,[14,15] "fast" consolidation rates were achieved by slip casting, and "slow" consolidation rates were achieved by low-speed centrifuging. As will be discussed in this paper, the differences in the means of particle motion (in slip casting, particles travel *with* the fluid, whereas in centrifugation, particles travel *through* the fluid) should preclude inferences regarding differences in consolidation rates.

The consolidation of suspensions containing highly anisometric particles, e.g., platelets, whiskers, and fibers, to high densities requires that the constituents are dispersed, adding to the importance of preventing segregation without agglomeration. Certainly, the prevailing mechanism of high solids fraction particle interactions can contribute to preventing segregation in such suspensions; however, other mechanisms should also contribute. No matter the consolidation rate (particle velocity), particles in a fluid are subject to hydrodynamic forces. The purpose of this paper is to demonstrate the importance of hydrodynamic particle interactions, i.e., interference drag or "drafting," on particle arrangement during consolidation. Hydrodynamic particle interactions are demonstrated in suspensions wherein the propensity for segregation was maximized (e.g., dispersed, dilute, and low viscosity), in order to exploit segregation for the formation of layered microstructures.[24,25]

II. Experimental Procedure

(1) Centrifugal Consolidation

Dilute (8 vol% solids), dispersed (pH 3), aqueous suspensions were prepared containing equal portions of Ce-ZrO_2 and fine Al_2O_3, and varying Al_2O_3-platelet contents (Table I). Hard agglomerates present in the commercial Ce-ZrO_2 powder were removed to aid in achieving high particle packing densities. An aqueous suspension of Ce-ZrO_2, at 10 vol% solids and pH 3 (with HNO_3), was dispersed by ultrasonication (Sonicator W-380, Heat Systems-Ultrasonics, Farmingdale, NY). After allowing the suspension to stand for 30 min, the remaining suspension was decanted. The removal of large agglomerates was confirmed by measuring the particle size distributions (Coulter LS 130 with fluid module), as shown in Fig. 1(a). The

J. W. Halloran—contributing editor

Manuscript No. 193003. Received December 5, 1994; approved April 12, 1995.
Supported by the National Science Foundation through Grant Nos. DMR-91-21948 and DMR-93-57496, and the Department of Basic Energy Sciences, the Midwest Superconductivity Consortium, Department of Energy Grant No. DE-FG02-90ER45427.

*Member, American Ceramic Society.

Table I. Starting Powders and Data

Powder	Solids in suspensions (vol%) #1	#2	#3	Density (g/cm^3)	Average particle size (μm)	Trade name, supplier
Al_2O_3 platelets	**5.0**	**12.5**	**20.0**	3.98*	1–25*,†	Elf Atochem, Paris, France
Fine Al_2O_3	47.5	43.8	40.0	3.98*	0.2*,†	AKP-50, Sumitomo Chemical, New York, NY
Fractionated Ce-ZrO_2	47.5	43.8	40.0	6.20*	2.6†	TZ-12Ce, Tosoh Ceramics Div., New Milford, CT

*From manufacturers' data. †Measured using a Coulter LS130 (with fluid module) particle size analyzer.

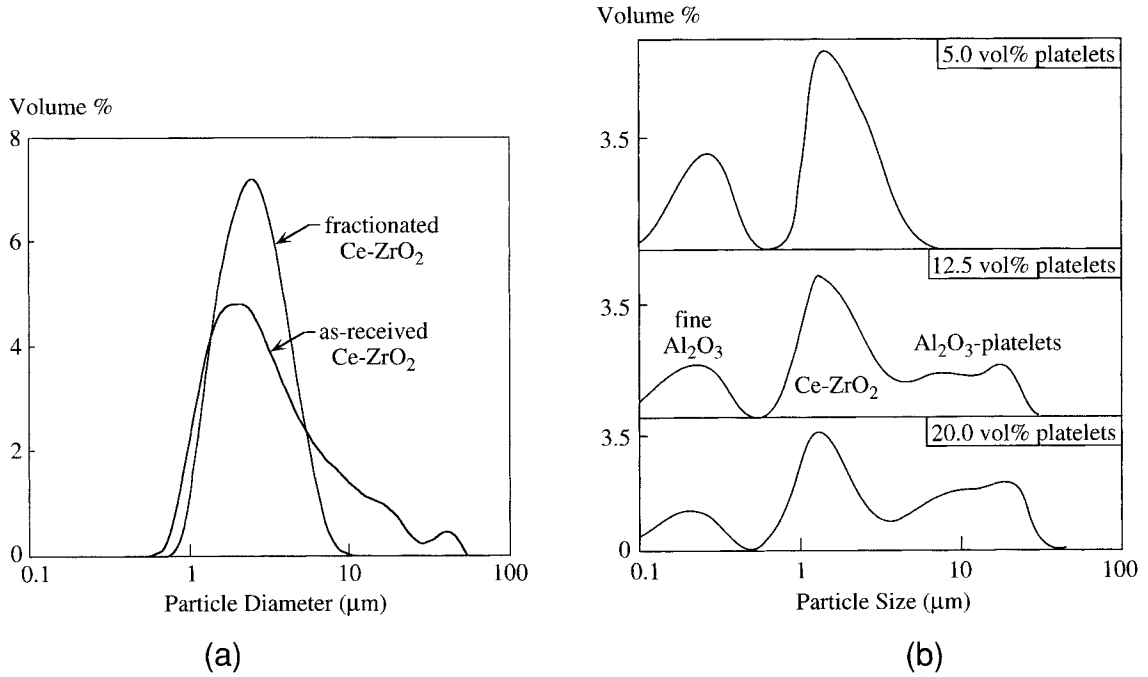

Fig. 1. Particle size distributions of, (a) the as-received Ce-ZrO_2 powder and the fractionated powder showing removal of hard agglomerates, and (b) the ternary Ce-ZrO_2/Al_2O_3/Al_2O_3-platelet suspensions showing the differences in size-scale and the effects of varying Al_2O_3-platelet content.

fractionated Ce-ZrO_2 suspension contained ~8 vol% solids and was maintained at pH 3. Aqueous suspensions of a fine Al_2O_3 and varying contents of hexagonal-shaped Al_2O_3 platelets (Fig. 2) were also prepared at 8 vol% solids and pH 3 (with HNO_3). The Al_2O_3 suspensions were mixed with appropriate amounts of the fractionated Ce-ZrO_2 suspension and again ultrasonicated, maintaining pH 3. The effects of the varying Al_2O_3-platelet contents were displayed by measuring the particle size distributions of the final suspensions (Fig. 1(b)).

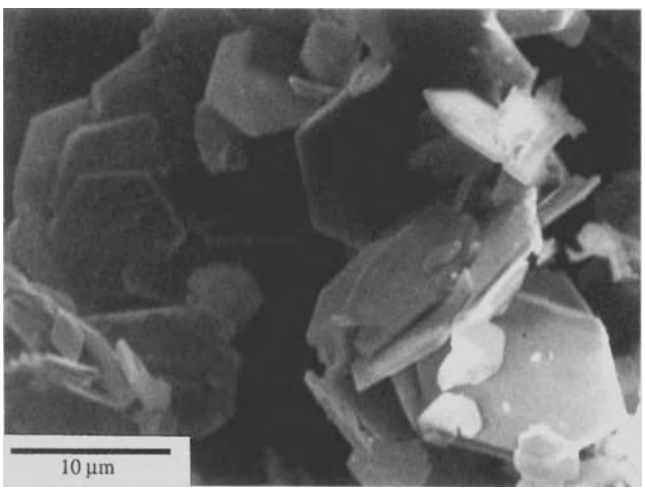

Fig. 2. SEM micrograph of the as-received, hexagonal-shaped Al_2O_3 platelets.

The ternary Ce-ZrO_2/Al_2O_3/Al_2O_3-platelet suspensions were centrifugally consolidated. Molds placed within the swinging buckets of a centrifuge (model CL, Damon/IEC, Needham Hts., MA) consisted of polyethylene tubes (2.5 cm inner diameter) with rubber balloons stretched and fastened over the bottom. Prior to consolidation, 4 mL of deionized water at pH 3 (using HNO_3) was placed in each of the four molds. The suspensions were consolidated by consecutively centrifuging 40 separate suspension additions (in each mold) of 0.25 mL at ~2150 g for 2 min per addition (Fig. 3). The pre-added water facilitated packing of layers of uniform thickness and provided long distances for particle displacement (and segregation) during consolidation. Also, since the solids content at the initiation of consolidation was always less than 0.5 vol%, changes in the solids fraction from suspension additions were negligible. The consolidation procedure required 1.5–2 h; therefore, care was taken to maintain the bulk suspension at pH 3 under constant mixing. At the completion of consolidation, the supernatants were poured off and the green bodies were dried. Specimens were sintered at 1600°C (800°C/h ramp) for 1 h, followed by ceramographic preparation and microstructural observation in a scanning electron microscope.

(2) Sedimentation Series

In order to further examine the consolidation behavior of the platelet-containing suspensions, suspensions were prepared containing a fine Al_2O_3 powder (AKP-30, Sumitomo Chemical, New York) with an average particle size of 0.4 μm, and varying Al_2O_3-platelet contents (12.5, 15.0, 17.5, 20.0, and 22.5 vol% of the solids). All suspensions contained 0.5 vol% solids and were ultrasonically dispersed at pH 3 (with HNO_3). Sonication and readjustment of pH were carried out successively until

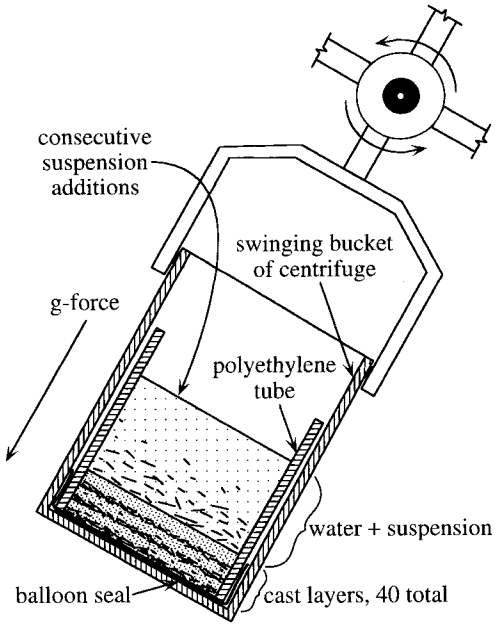

Fig. 3. Schematic representation (not to scale) of centrifugal consolidation of segregated layers in the swinging bucket of a centrifuge.

the pH no longer deviated from pH 3 after sonication. The suspensions were placed in each of five graduated cylinders, containing 10 mL of suspension per cylinder. The suspensions were allowed to stand for 2 days, during which sedimentation was observed and photographically recorded.

III. Results

(1) Centrifugal Consolidation

The microstructures resulting from centrifugal consolidation reveal that the 5.0 and 12.5 vol% platelet suspensions segregated, while the 20.0 vol% platelet suspension did not (Fig. 4). The differences in the consolidation behavior were further demonstrated by observing the supernatant liquid at the completion of consolidation. In the suspensions that segregated, some degree of cloudiness (greatest for the 5.0 vol% platelet suspension) was observed in the supernatants, corresponding to fine particles that remained suspended and dispersed. Conversely, the supernatants of unsegregated composites were clear, indicating that all particles had consolidated. Given the background on conventional mechanisms of preventing segregation and the conditions of the experiments in this study, segregation was expected in all three suspensions. However, the same consolidation behavior was repeatedly observed in similar experiments with platelet loadings near 20.0 vol%.

(2) Sedimentation Series

The purpose of the sedimentation series was to examine in more detail the apparent change in consolidation behavior from 12.5 to 20.0 vol% platelet contents observed in centrifugal consolidation experiments. Additionally, the sedimentation series excluded ZrO_2 to eliminate the possibility of heteroflocculation or heterocoagulation, and allowed comparison of gravitational sedimentation to that of the high g-forces (and higher consolidation rate) in the centrifuge.

Photographs of the sedimentation series (Fig. 5) show remarkable correlation to the centrifugation experiments. As expected, the large noncolloidal platelets were dispersed but not stable. Thus, platelets began to settle out of suspension immediately, and a layer of sediment could be seen in all suspensions after only 4–6 min. Unfortunately, the cloudiness of the low platelet content suspensions at early times made the initial sediment (height shown by arrows in Fig. 5) difficult to show photographically. Nevertheless, while an initial platelet

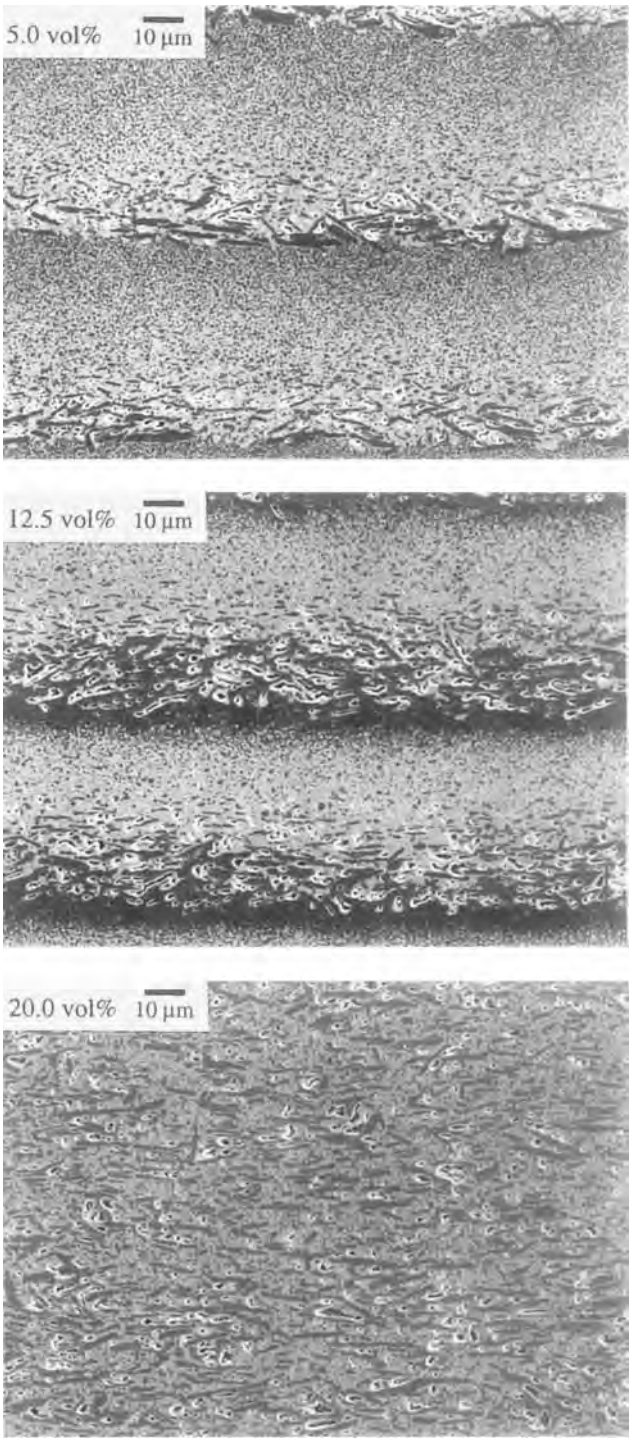

Fig. 4. SEM micrographs showing 5.0, 12.5, and 20.0 vol% Al_2O_3-platelet composite microstructures after sintering 1 h at 1600°C.

sediment formed at the same time in all suspensions, there was an obvious difference in sedimentation behavior across the series. Just after the initial sediment formed in the 20.0 and 22.5 vol% platelet suspensions, a distinct boundary was visible between the sediment and the remaining suspension (Fig. 5). With lower platelet contents, the boundary was increasingly less distinct. Accordingly, the remaining suspension was relatively clear for 20.0 and 22.5 vol% platelet suspensions and cloudy for lower platelet contents. The remainder of the 12.5 and 15.0 vol% platelet suspensions maintained a high degree of cloudiness for the remaining 2 days of the experiment. After 2 days, all suspensions still had pH<4; thus, the suspensions

remained dispersed, and time-dependent flocculation or coagulation was eliminated.

IV. Discussion

Conventional mechanisms for preventing segregation in suspension processing fail to explain the consolidation behavior observed in the present investigation. Since the solids content was maintained at 8 vol% in the bulk suspensions and less than 0.5 vol% at the initiation of consolidation over long settling distances, the high solids loading mechanism can obviously be ruled out. Similarly, viscosity is clearly minimal in a low solids content, aqueous dispersion. At pH 3, electrokinetic measurements show that Al_2O_3 and ZrO_2 have nearly equal positive zeta potentials;[10,14] therefore, flocculation and heteroflocculation are considered highly improbable.[26] Furthermore, there is no microstructural evidence of any platelet agglomeration or preferred association between the different constituents. Even if all the platelets were to become agglomerated with a single monolayer of the smaller particles, greater than 70% of the smaller particles would remain and segregation would still be expected. For these reasons, some other mechanism must be contributing.

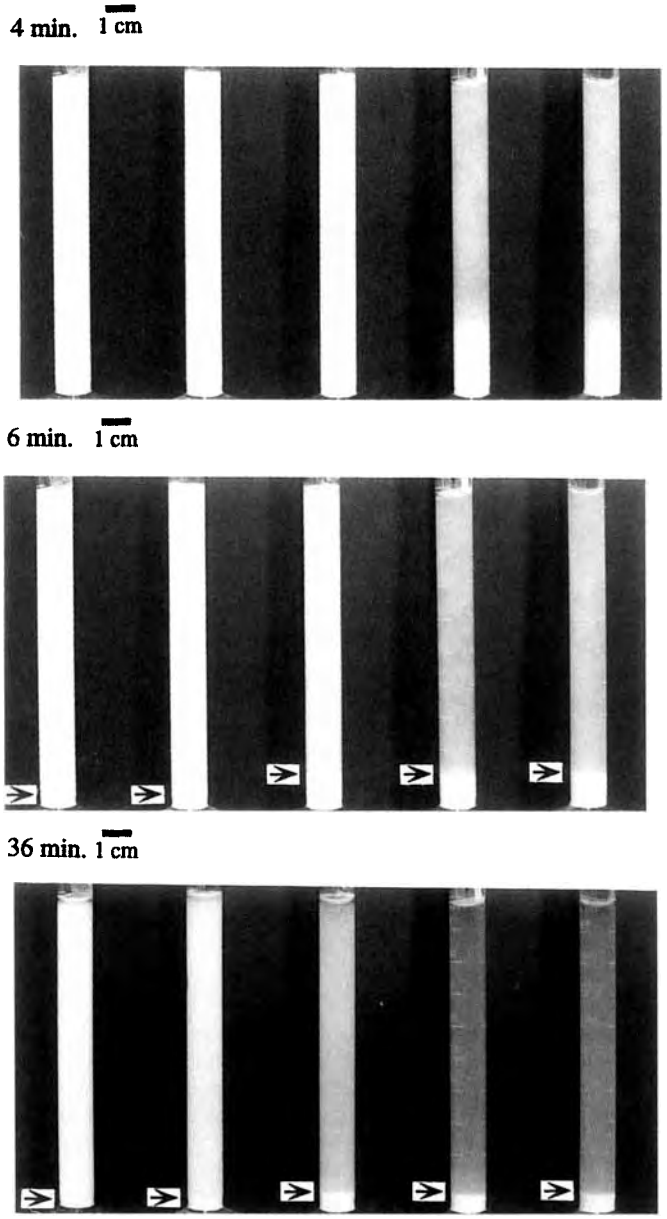

Fig. 5. Photographs of the sedimentation series after 4, 6, and 36 min. Suspensions contained 0.5 vol% solids with varying Al_2O_3-platelet contents (left to right) of 12.5, 15.0, 17.5, 20.0, and 22.5 vol% of solids. Arrows indicate the height of the initial sediment.

(1) Hydrodynamic Forces

Any solid object traveling in a fluid medium produces hydrodynamic forces. Drag is any force (F_D) that opposes motion of a body in a fluid medium and is exerted on the body by the medium (for a review of hydrodynamic drag, see Ref. 27). Two types of drag exist: friction drag and pressure drag. Friction drag results from forces tangential to body surfaces and is given as $F_D = \int_{surface} \tau_W \cdot \partial A$, where τ_W is the shear stress and A is the area under friction. Pressure drag results from forces normal to the body surface created by local pressure variations at the body surface. Pressure drag is derived as $F_D = \int_{surface} P \cdot \partial A$, where P is the local pressure at the surface and A is the area normal to flow. For a thin plate (or platelet), friction drag can be assumed negligible relative to pressure drag, so that drag is only a function of the pressure over the surface normal to flow.

Variation in local pressure around the body surface is created by flow separation. For laminar flow, the point of separation is dependent on object shape only. Laminar flow lines are parallel and velocity gradients may exist, but velocities are steady. In order for flow to remain attached, the pressure gradient around the sharp edges of a bluff body (e.g., platelet) must approach infinity from the edge to the rear stagnation point. Thus, the boundary layer and external flow are separated from a platelet at its edges, and a wake is produced (Fig. 6).

The Reynolds number (Re) is a nondimensional parameter used to describe flow in terms of the flow velocity, a characteristic length, and the fluid's kinematic viscosity (ν). For the flow of hexagonal platelets, the Reynolds number is defined as $Re = l \cdot v_t/\nu$, where the characteristic length (l) is the long dimension of the face, and the flow velocity is the terminal particle velocity (v_t). The drag coefficient (C_D) nondimensionally quantifies the extent of drag relative to the flow conditions (Re), and the size and shape of the body. The drag coefficient is given as,

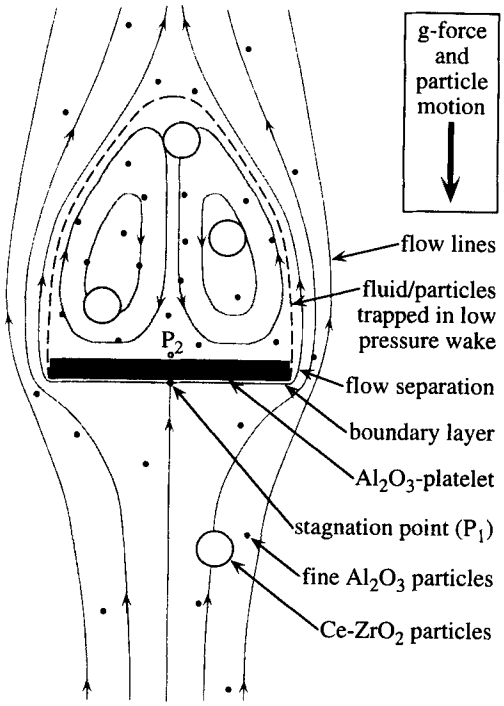

Fig. 6. Schematic representation of particle drafting as a means of preventing segregation. Note that the relative particle sizes shown are in scale with those used in the experiments.

$$C_D = \frac{F_D}{qA} = \frac{F_D}{\frac{1}{2}\rho v_t^2 A}$$

where q is the dynamic pressure, ρ is the fluid density, v_t is the terminal (steady-state) velocity of the body, and A is the area of the body normal to flow. The pressure coefficient (C_p) is another nondimensional quantity used to relate the variation in the local pressure (P) at the body surface to the free flow pressure (P_∞) in the undisturbed fluid. The pressure coefficient is given by

$$C_p = \frac{\Delta P}{q} = \frac{P - P_\infty}{\frac{1}{2}\rho v_t^2}$$

When flow separation occurs, C_p is positive where the boundary layer is attached (i.e., in front of the platelet in Fig. 6) and negative where the boundary layer is separated (i.e., behind the platelet). Thus, a region of relative low pressure ($P_1 >> P_2$ in Fig. 6) is expected in the wake of a traveling body. Unfortunately, the magnitude and distribution of the local pressure variations cannot be calculated. The pressure distribution (and C_p) for viscous flow around objects can be determined only through modeling[28–34] or experiment.[28–30] However, since C_p is a function of particle shape and velocity, the size and magnitude of the relative low pressure region behind a body (given that boundary layer separation occurs) will scale with C_D, which can be determined.

The drag coefficient was determined as a function of the Reynolds number characterizing the flow, for varying hexagonal platelet aspect ratios (Fig. 7). A detailed analysis of the calculations used is given in the Appendix. As shown in Fig. 7, increasing the platelet aspect ratio results in greater drag over the entire range of Reynolds numbers. For increasing Reynolds number, drag decreases to a minimum, after which it increases slightly and becomes constant. Thus, laminar flow predominates up to Re $\approx$ 60–100, and the wake becomes fully turbulent by Re $\approx$ 500–1000, depending on platelet aspect ratio. Within this context, the nature of platelet motion can be described based upon experimental observations.[35–38] For Re $<$ 1, flow is steady and a platelet does not orient relative to flow, maintaining any initial orientation. However, for 1 $<$ Re $<$ 100, platelets will orient perpendicular to the direction of flow (Fig. 6), while flow remains steady. In this region, the wake length has also been shown to be directly proportional to Re.[30,32–34] At Re $>$ 100, vortex shedding at the separation point is evidence of unsteady flow in the transition from laminar to turbulent flow. Unsteady flow for a platelet is generally observed as wobbling or pitching motions and can even include spinning for platelets with a large enough aspect ratio at high Reynolds numbers (Re $>$ 500).

(2) Interference Drag

In the preceding discussion on hydrodynamic forces, only single, noninteracting particles are considered. The effects of particle interactions on hydrodynamic forces, however, are less understood. Others have observed a tendency for particles to settle in hydrodynamic "clusters,"[21] but no hydrodynamic explanation has been discussed. The nature of hydrodynamic particle interactions is determined by the size, shape, separation distance, orientation relative to flow, arrangement, and velocity of the involved particles. Hydrodynamic particle interactions occur when the flow disturbance (nonrectilinear flow lines) created by one particle interacts with that of another particle. Interference drag considers the effects of hydrodynamic particle interactions on drag for specific particle arrangements.

Interference drag can be modeled by considering a small spherical particle (body 2) behind a platelet (body 1), near each other without touching (Fig. 8). The combined drag force of the two particle system ($F_{D,sys} = F_{D,1} + F_{D,2}$) depends only on the separation distance of the particles relative to the size of the platelet wake for a specified Reynolds number. Thus, for a fixed

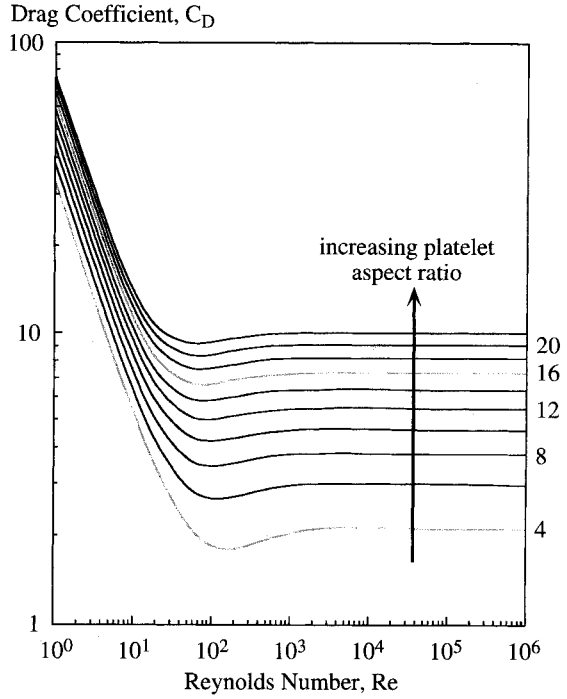

Fig. 7. The drag coefficient of hexagonal platelets of varying aspect ratio as a function of the Reynolds number characterizing the flow.

platelet shape, the size of the platelet wake depends only on the platelet size. The interference drag (ΔF_D) is defined as

$$\Delta F_D = F_{D,sys} - (F_{D,1}^\infty + F_{D,2}^\infty) = (F_{D,1} + F_{D,2}) - (F_{D,1}^\infty + F_{D,2}^\infty)$$

where $F_{D,1}^\infty$ and $F_{D,2}^\infty$ are the drag forces on the isolated individual bodies under free-flow conditions. Likewise, for n multiple particles within the wake of a single platelet (assuming no platelet/platelet interactions and that interactions between particles are negligible compared to platelet/particle interactions),

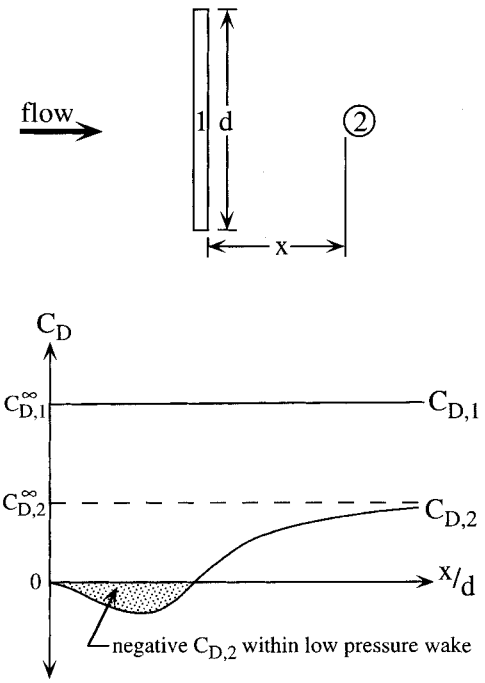

Fig. 8. Schematic and graphical representation of the effects of interference drag, showing the drag coefficients (C_D) of a platelet and a smaller spherical particle versus separation distance normalized to the platelet size (x/d). The superscript, ∞, denotes behavior under free-flow conditions.

$$\Delta F_D = F_{D,sys} - (F^{\infty}_{D,platelet} + \sum_{i=1}^{n} F^{\infty}_{D,i})$$

$$= (F_{D,platelet} + \sum_{i=1}^{n} F_{D,i}) - (F^{\infty}_{D,platelet} + \sum_{i=1}^{n} F^{\infty}_{D,i})$$

Interference can decrease ($\Delta F_D < 0$) or increase ($\Delta F_D > 0$), the drag of the system relative to the sum of the individual components under free-flow conditions. As the individual drag forces approach free-flow values, the interference drag becomes zero and particles are not interactive. A decreased drag on the system ($\Delta F_D < 0$) occurs when the particle is within the platelet wake such that the platelet drag is relatively undisturbed and the particle drag is less than for free flow. The particle drag is decreased due to the relative low pressure within the platelet wake created by flow separation. An increased drag on the system ($\Delta F_D > 0$) can occur when the particle interferes with the platelet wake such that the wake size is increased, increasing both the particle and platelet drag.[27–29]

The effects of interference drag on the drag coefficients of the individual bodies are shown in Fig. 8. The drag coefficient of the particle ($C_{D,2}$) is lower than for free-flow conditions ($C^{\infty}_{D,2}$) because of decreased dynamic pressure within the wake of the platelet. As the distance (x) between the bodies is decreased or the size of the platelet (d) is increased, the drag coefficient of the particle ($C_{D,2}$) decreases, while that of the platelet ($C_{D,1}$) varies negligibly. Conversely, increasing distance and decreasing size of the platelet allow the particle drag coefficients to approach the free-flow values.

(3) Particle Drafting

Practical illustrations of interference drag are prevalent. In sailboat racing, a common strategy is to maneuver between the direction of the wind and the competitors' sails such that wind is kept out of the competitors' sails. In auto racing (particularly stock car racing), competitors often maneuver directly behind one another to achieve higher speeds or conserve fuel ("drafting"). Likewise, in platelet–particle drafting, much smaller particles can achieve average velocities equal to those of large platelets when positioned in the platelet wake.

The experimental results and analysis of hydrodynamic forces presented up to this point lead to the proposal of particle drafting as a mechanism for preventing segregation. A model physical description of particle drafting is shown schematically in Fig. 6. Smaller particles are "carried" in the low-pressure wake of a larger particle (i.e., platelet). The small particles appear to be "carried" because of higher than normal (for free flow) velocities due to a lower resistance to flow (drag) in the low-pressure wake. Thus, particle drafting can occur for either laminar or turbulent flow. In laminar flow, the fluid and particles in the low-pressure wake behind the platelet remain trapped (no "mixing"). In turbulent flow, however, fluid and particles are periodically released and captured, due to velocity fluctuations within the turbulent wake.

The sedimentation series suggests that particle drafting occurs under flow conditions which are clearly laminar. On the other hand, the higher particle velocities in centrifugal consolidation lead to higher Reynolds numbers that could be in the transition between laminar and fully turbulent flow. If the estimated terminal velocity of a platelet is reached (calculation of particle velocity is ambiguous without measurements), the maximum Reynolds number achievable by the centrifugal consolidation experiments is approximately 25. Thus, it is reasonable to assume that flow was predominantly laminar, even for the high g-loads of centrifugal consolidation, and Re $\approx$ 1–25 is predicted for platelets during consolidation. This estimation points out, however, that turbulence effects and accurately *measured* particle velocity are of prime concern for an understanding of particle drafting. Furthermore, factors could be correlated to changes in the wake pressure distribution determined through modeling or fluid channel experiments. Determination of the critical number of particles that can "draft" in the wake of a platelet as a function of platelet aspect ratio, particle size, and Reynolds number would be advantageous.

The experimentally observed dependence of segregation on the platelet volume fraction of solids can be explained by considering the relative amounts of the different particle constituents. Because of repulsive interparticle surface forces, the addition of particles to the wake of a platelet must eventually result in another being forced out of the wake. Thus, a single platelet can "carry" only a finite volume of smaller particles in its wake. Based on experimental flow visualizations,[34,35,38] the approximate shape and volume of the wake behind a platelet for stable flow is shown schematically in Fig. 6. The volume of the wake behind an isolated, noninteracting platelet is approximately 10 times the volume of the platelet. If segregation is to be prevented, the volume of smaller particles per platelet in the suspension must fit within the wake. For a given platelet content, the volume ratio of particles per platelet is approximately seven for 12.5 vol% platelets and four for 20.0 vol% platelets. Thus, in the suspensions that did not segregate (20.0 and 22.5 vol% platelets), platelets could "carry" a maximum of four times their volume in the wake. If the wake was 10 times the platelet's volume (assuming the size of the wake was not significantly changed by adding smaller particles), the wake would contain ~40 vol% solids, which corresponds to the maximum solids loading achievable when preparing bulk suspensions.

Finally, other interactions are also taking place: platelets drafting platelets, fine Al_2O_3 drafting larger Ce-ZrO_2, interactions within a wake, the upward flow of displaced fluid, etc. Also, the possibility of surface force contributions (including platelet surface energy anisotropy or weak flocculation) should not be neglected, although surface forces act primarily over distances of nanometers, while hydrodynamic interactions act over large volumes (up to 30 times the platelets volume) of fluid. Comprehensive analysis of hydrodynamic particle interactions is a complex, three-dimensional, and many-bodied problem. Thus, practical analysis is needed and justifies the use of simplifying assumptions to determine fundamental relationships. The simplified analysis presented here captures the basic features, is consistent with experimental results, and is a starting point for more detailed analysis.

V. Summary

Centrifugal consolidation of dilute, dispersed, multicomponent suspensions with a wide range of particle sizes revealed consolidation behavior unexplained by conventional mechanisms. Despite conditions favoring segregation, phase and size segregation did not occur in suspensions with sufficient contents of anisometric noncolloidal particles. Particle drafting, based on the hydrodynamic principle of interference drag, is proposed and supported as a mechanism responsible for segregation prevention. In interference drag, particles located within the low-pressure wake of a bluff body achieve higher than normal (for free-flow conditions) velocities due to the lower drag. Thus, particles can be "carried" within the wake of a moving bluff body.

The effects of hydrodynamic particle interactions on consolidation behavior should not be overlooked. In dispersed suspensions containing noncolloidal particles, the consolidation behavior can be mostly dependent on hydrodynamic forces, rather than surface forces. Furthermore, even in systems where interparticle surface forces dominate, when interparticle surface forces reach a level of high predictability, the next step is to understand and control hydrodynamic particle interactions.

APPENDIX

Calculation of the Drag Coefficient for Platelets

Methods for predicting drag coefficients that account for nonspherical particle shapes are reviewed by Thompson and

Clark.[40] The degree of dimensional anisotropy of nonspherical particles is expressed by different shape factors, sphericity[41–43] being the most widely utilized. Sphericity (Ψ) is ideal for describing smooth, geometric particles (e.g., platelets) and is defined by the expression

$$\Psi = \frac{A_s}{A_p}$$

where A_s is the surface area of a sphere with volume equivalent to that of the particle, and A_p is the surface area of the particle. Thus, the sphericity of smooth, uniform hexagonal platelets is given by

$$\Psi_{hex} = \frac{\pi\left(\frac{9\sqrt{3}tl^2}{2\pi}\right)^{2/3}}{1.5\sqrt{3}l^2 + 3lt} = \frac{\pi\left(\frac{9\sqrt{3}a^2}{2\pi}\right)^{2/3}}{1.5\sqrt{3}a^2 + 3a}$$

where l is the long dimension of the face and t is the thickness. If a constant unit thickness is taken as 1 μm, the sphericity can be easily determined in terms of platelet aspect ratio ($a = l/t = 1$). Haider and Levenspiel[44] formulated an expression for the drag coefficient (C_D) as a function of particle sphericity and Reynolds number (Re). The expression is that of a curve fit to model substantial experimental data[35–38] and is defined as

$$C_D = \frac{24}{\mathrm{Re}}(1 + A\mathrm{Re}^B) + \left[\frac{C}{1 + D/\mathrm{Re}}\right]$$

where A, B, C, and D are the following functions of sphericity:

$$A = \exp(2.3288 - 6.4581\Psi + 2.4486\Psi^2)$$

$$B = 0.0964 + 0.5565\Psi$$

$$C = \exp(4.905 - 13.8944\Psi + 18.4222\Psi^2 - 10.2599\Psi^3)$$

$$D = \exp(1.4681 + 12.258\Psi - 20.73222\Psi^2 + 15.8855\Psi^3)$$

The preceding analysis is justified by the *law of dynamic similitude*, which states that equal Reynolds numbers yield equal drag coefficients for similar shapes (or sphericity) regardless of size. The analysis is also advantageous in that C_D is correlated to experimental data rather than theory, and the ambiguous calculation of particle velocity is avoided.

Acknowledgments: The authors thank E. B. Slamovich for advice in preparing the manuscript, B. Jarosinski (Praxair Surface Technologies, Indianapolis, IN) for particle size measuremens, and J. Blendell (NIST) for providing the Atochem Al_2O_3 platelets.

References

[1]W. C. Moffatt, H. P. White, and H. K. Bowen, "Production of Alumina–Zirconia Composite Ceramics by Nonsolvent Flocculation of Polymer-Containing Powder Dispersions"; pp. 645–53 in Ceramic Transactions, Vol. 1, *Ceramic Powder Science II*. Edited by G. L. Messing, E. Fuller, and H. Hausner. American Ceramic Society, Westerville, OH, 1988.

[2]F. F. Lange, "Forming a Ceramic by Flocculation and Centrifugal Casting," U.S. Pat. No. 4 624 808, Nov. 25, 1986.

[3]B. V. Velamakanni and F. F. Lange, "Effect of Interparticle Potentials and Sedimentation on Particle Packing Density of Bimodal Particle Distribution during Pressure Filtration," *J. Am. Ceram. Soc.*, **74** [1] 166–72 (1991).

[4]P. E. Debély, E. A. Barringer, and H. K. Bowen, "Preparation and Sintering Behavior of Fine-Grained Al_2O_3–SiO_2 Composite," *J. Am. Ceram. Soc.*, **68** [3] C-76–C-78 (1985).

[5]F. F. Lange and K. T. Miller, "A Colloidal Method to Ensure Phase Homogeneity in β″-Al_2O_3/ZrO_2 Composite Systems," *J. Am. Ceram. Soc.*, **70** [12] 896–900 (1987).

[6]T. Kimura, Y. Kaneko, and T. Yamaguchi, "Consolidation of Alumina–Zirconia Mixtures by a Colloidal Process," *J. Am. Ceram. Soc.*, **74** [3] 625–32 (1991).

[7]B. V. Velamakanni, J. C. Chang, F. F. Lange, and D. S. Pearson, "New Method for Efficient Colloidal Packing via Modulation of Repulsive Lubricating Hydration Forces," *Langmuir*, **6** [7] 1323–25 (1990).

[8]J. C. Chang, B. V. Velamakanni, F. F. Lange, and D. S. Pearson, "Centrifugal Consolidation of Al_2O_3 and Al_2O_3/ZrO_2 Composite Slurries vs Interparticle Potentials: Particle Packing and Mass Segregation," *J. Am. Ceram. Soc.*, **74** [9] 2201–204 (1991).

[9]S. Baik, A. Bleier, and P. F. Becher, "Preparation of Al_2O_3/ZrO_2 Composites by Adjustment of Surface Chemical Behavior"; pp. 791–800 in *Better Ceramics through Chemistry II*. Edited by C. J. Brinker, D. E. Clark, and D. R. Ulrich. Materials Research Society, Pittsburgh, PA, 1986.

[10]A. Bleier and C. G. Westmoreland, "Effects of pH and Particle Size on the Processing and the Development of Microstructure in Alumina–Zirconia Composites," *J. Am. Ceram. Soc.*, **74** [12] 3100–11 (1991).

[11]G. L. Messing and M. Kumagai, "Low-Temperature Sintering of Seeded Sol–Gel Derived, ZrO_2-Toughened Al_2O_3 Composites," *J. Am. Ceram. Soc.*, **72** [1] 40–44 (1989).

[12]E. Beylier, R. L. Pober, and M. J. Cima, "Centrifugal Casting of Ceramic Components"; pp. 529–36 in Ceramic Transactions, Vol. 12, *Ceramic Powder Science III*. Edited by G. L. Messing, S. Hirano, and H. Hausner. American Ceramic Society, Westerville, OH, 1990.

[13]W. Huisman, T. Graule, and L. J. Gauckler, "Centrifugal Slip Casting of Zirconia (TZP)," *J. Eur. Ceram. Soc.*, **13**, 33–39 (1994).

[14]M. D. Sacks, H. W. Lee, and O. E. Rojas, "Suspension Processing of Al_2O_3/SiC Whisker Composites," *J. Am. Ceram. Soc.*, **71** [5] 370–79 (1988).

[15]M. D. Sacks, H. W. Lee, and O. E. Rojas, "Suspension Processing of SiC Whisker-Reinforced Ceramic Composites"; see Ref. 1, pp. 440–51.

[16]M. J. Lockett and H. M. Habbooby, "Differential Settling of Two Particle Species in a Liquid," *Trans. Inst. Chem. Eng.*, **51**, 281–92 (1973).

[17]R. A. Williams, W. B. K. Amarasinghe, S. J. R. Simons, and C. G. Xie, "Sedimentation Behavior of Complex Polydisperse Suspensions," *Powder Technol.*, **65**, 411–32 (1991).

[18]M. A. Hassen and R. H. Davis, "Effects of Particle Interactions on the Determination of Particle Size Distribution by Sedimentation," *Powder Technol.*, **58**, 285–89 (1989).

[19]R. H. Davis and M. A. Hassen, "Spreading of the Interface at the Top of a Polydisperse Sedimenting Suspension," *J. Fluid Mech.*, **196**, 107–34 (1988).

[20]J. E. Bhatty and D. Dollimore, "Sedimentation Behavior of Polydispersed Suspensions"; pp. 77–85 in Particulate and Multiphase Processes, Vol. 3, *Colloidal and Interfacial Phenomena*. Edited by T. Ariman and T. N. Veziroglu. Hemisphere Publishing, Washington, D.C., 1985.

[21]J. I. Bhatty, "Clusters Formation during Sedimentation of Dilute Suspensions," *Sep. Sci. Technol.*, **21** [90] 953–67 (1986).

[22]M. D. Sacks, "Rheological Science in Ceramic Processing"; pp. 522–38 in *Science of Ceramic Chemical Processing*. Edited by L. L. Hench and D. R. Ulrich. Wiley, New York, 1986.

[23]J. C. Chang, F. F. Lange, and D. S. Pearson, "Viscosity and Yield Stress of Alumina Slurries Containing Large Concentrations of Electrolyte," *J. Am. Ceram. Soc.*, **77** [1] 19–26 (1994).

[24]R. K. Roeder, K. J. Bowman, and K. P. Trumble, "Texture and Microstructure Development in Al_2O_3-Platelet Reinforced Ce-ZrO_2/Al_2O_3 Laminates Produced by Centrifugal Consolidation," *Textures Microstruct.*, **24**, 43–52 (1995).

[25]R. K. Roeder, K. J. Bowman, and K. P. Trumble, unpublished results.

[26]I. A. Aksay, F. F. Lange, and B. I. Davis, "Uniformity of Al_2O_3–ZrO_2 Composites by Colloidal Filtration," *J. Am. Ceram. Soc.*, **66** [10] C-190–C-192 (1983).

[27]S. F. Hoerner, *Fluid-Dynamic Drag*. S. F. Hoerner, Brick Town, NJ, 1965.

[28]F. F. Grinstein, J. P. Boris, and O. M. Griffin, "Passive Pressure-Drag Control in a Plane Wake," *AIAA J.*, **29** [9] 1436–42 (1991).

[29]A. Roshko, "On the Wake and Drag of Bluff Bodies," *J. Aerosol. Sci.*, **22** [2] 124–32 (1955).

[30]A. Acrivos, L. G. Leal, D. D. Snowden, and F. Pan, "Further Experiments on Steady Separated Flows past Bluff Objects," *J. Fluid Mech.*, **34**, 25–48 (1968).

[31]M. Ray, "On the Problem of a Circular Disk in Viscous Fluid," *Philos. Mag. S.7*, **21** [141] 546–64 (1936).

[32]F. T. Smith, "A Structure for Laminar Flow past a Bluff Body at a High Reynolds Number," *J. Fluid Mech.*, **155**, 175–91 (1985).

[33]J. D. Hudson and S. C. R. Dennis, "The Flow of a Viscous Incompressible Fluid past a Normal Flat Plate at Low Reynolds Numbers: The Wake," *J. Fluid Mech.*, **160**, 369–83 (1985).

[34]D. B. Ingham, T. Tang, and B. R. Morton, "Steady Two-Dimensional Flow through a Row of Normal Flat Plates," *J. Fluid Mech.*, **210**, 210, 281–302 (1989).

[35]W. W. Willmarth, N. E. Hawk, and R. L. Harvey, "Steady and Unsteady Motions and Wakes of Freely Falling Disks," *Phys. Fluids*, **7** [2] 197–208 (1964).

[36]E. S. Pettyjohn and E. B. Christianson, "Effect of Particle Shape on the Free-Settling Rates of Isometric Particles," *Chem. Eng. Prog.*, **44** [2] 157–72 (1948).

[37]V. J. Schmeidel, "Experimentelle Untersuchungen über die Fallbewegung von Kugeln und Scheiben in Reibenden Flüssigkeiten," *Phys. Z.*, **29**, 593–610 (1928).

[38]L. Squires and W. Squires Jr., "The Sedimentation of Thin Discs," *Trans. Am. Inst. Chem. Eng.*, **33** [1] 1–12 (1937).

[39]D. Marshall and T. E. Stanton, "On the Eddy System on the Wake of Flat Circular Plates in Three Dimensional Flow," *Proc. R. Soc.*, **A130**, 295–301 (1931).

[40]T. L. Thompson and N. N. Clark, "A Holistic Approach to Particle Drag Prediction," *Powder Technol.*, **67**, 57–66 (1991).

[41]H. Wadell, "Volume, Shape, and Roundness of Rock Particles," *J. Geol.*, **40**, 443–51 (1932).

[42]H. Wadell, "Sphericity and Roundness of Rock Particles," *J. Geol.*, **41**, 310–31 (1933).

[43]H. Wadell, "The Coefficient of Resistance as a Function of Reynolds Number for Solids of Various Shapes," *J. Franklin Inst.*, **217**, 459–90 (1934).

[44]A. Haider and O. Levenspiel, "Drag Coefficient and Terminal Velocity of Spherical and Nonspherical Particles," *Powder Technol.*, **58**, 63–70 (1989). □